Cardiovascular Research (2013) **100**, 241–251
doi:10.1093/cvr/cvt192

Cardiac stem cells with electrical stimulation improve ischaemic heart function through regulation of connective tissue growth factor and miR-378

Sun Wook Kim[1], Ha Won Kim[2], Wei Huang[2], Motoi Okada[2], Jeffrey A. Welge[3], Yigang Wang[2], and Muhammad Ashraf[2]*

[1]Department of Molecular and Cellular Physiology, [2]Department of Pathology and Laboratory Medicine, Division of Regenerative Medicine; and [3]Department of Psychiatry and Behavioral Neuroscience, University of Cincinnati, 231 Albert Sabin Way, Cincinnati, OH 45267, USA

Received 12 October 2012; revised 30 July 2013; accepted 6 August 2013; online publish-ahead-of-print 25 September 2013

Time for primary review: 21 days

Aims In this study, we investigated whether pre-conditioning (PC) by electrical stimulation (EleS) induces cytoprotective effect on cardiac stem cells (CSCs) and determined its underlying molecular mechanisms.

Methods and results Sca-1$^+$ CSCs were isolated from male C57BL6 mice (12 weeks) hearts. PC of CSCs with EleS (^{EleS}CSCs) was carried out for 3 h at 1.5 V followed by exposure to 300 μM H_2O_2 for 5 h. Cytoprotective effects and cell adhesion ability were significantly increased by EleS as evaluated by transferase-mediated dUTP nick-end labelling (TUNEL), lactate dehydrogenase (LDH) release assay, and adhesion assay. EleS increased phosphorylation of AKT, focal adhesion kinase (FAK), and glycogen synthase kinase (GSK3β), as well as decreased caspase-3 cleavage. Interestingly, inhibition of AKT or FAK abolished the pro-survival effects of EleS. We found that connective tissue growth factor (*Ctgf*) was responsible for EleS-induced CSC survival and adhesion. The survival rate of ^{EleS}CSCs after transplantation in the infarcted myocardium was significantly increased together with improvement in cardiac function. Importantly, knockdown of *Ctgf* abolished EleS-induced cytoprotective effects and recovery of cardiac function. Furthermore, we identified miR-378 as a potential *Ctgf* regulator in ^{EleS}CSCs.

Conclusion EleS enhanced CSC survival *in vitro* and *in vivo* as well as functional recovery of the ischaemic heart through an AKT/FAK/CTGF signalling pathway. It is suggested that Ctgf and miR-378 are novel therapeutic targets for stem cell-based therapy.

Keywords Electrical stimulation • Survival • Ischaemic heart • CTGF • miR-378

1. Introduction

Stem cell therapy has emerged as a promising strategy for repair of injured myocardium. However, this approach suffers from massive death of transplanted stem cells in the infarcted heart. Various strategies have been adopted to prime donor stem cells for improving their survival post-engraftment. Pre-conditioning (PC) of stem cells either through a brief period of ischaemia/anoxia or treatment with alternative mimetic improves their post-engraftment survival and differentiation characteristics.[1–3] Ischaemic PC (IPC) with repeated cycles of intermittent hypoxia/re-oxygenation increased stem cell survival under subsequent exposure to anoxia after transplantation via miR-210 overexpression by targeting caspase 8-associated protein.[3] Pharmacological PC with mitochondrial potassium channel opener such as diazoxide suppresses apoptosis and promotes proliferation.[1,4] Similarly, up-regulation of pro-survival gene with angiogenic growth factor delivery[5] or overexpression of AKT increases stem cell survival under the ischaemic heart condition.[6] It has been reported that genetically modified myocytes with heat shock protein 72 (Hsp72) or Hsp20 were more resistant to the hypoxic condition.[7,8]

Recently, it has been reported that electrical stimulation (EleS) significantly increased proliferation[9–11] as well as differentiation in mesenchymal stem cells[12] and embryonic stem cells.[13–15] EleS activates phosphoinositide 3-kinase/AKT signalling pathway that plays a crucial role in cell survival.[16] Another report showed that EleS-mediated cytoprotection is due to vascular endothelial growth factor secretion from human umbilical

* Corresponding author. Tel: +1 513 234 4485; fax: +1 513 558 2141, Email: ashrafm251@gmail.com

vascular endothelial cells.[17] Taken together, these studies suggest that EleS-induced cytoprotection could be exploited to mitigate ischaemic injury.

The heart generates a constant electrical field, the effect of which has not been explored in stem cells prior to transplantation. EleS shares several beneficial attributes with IPC and besides being protective, and promotes cell proliferation[10–12] and differentiation.[13–15] However, there is no known report regarding the role of PC with EleS in stem cell survival and adhesion. In this study, we demonstrated that EleS provides PC effects on the survival of cardiac stem cells (CSCs) through an increase in cell adhesion via focal adhesion kinase (FAK) activation, and releasing connective tissue growth factor (CTGF) by miR-378 down-regulation.

2. Methods

2.1 Animals

All animal experiments conformed to The Guidelines for Care and Use of Laboratory Animals published by the US National Institutes of Health (NIH Publication No. 85-23, revised 1985), and all protocols of animal experiments were approved by the Institutional Animal Care and Use Committee, University of Cincinnati.

2.2 Isolation of Sca-1$^+$ CSCs

C57BL6 mice (Harlan) were used for isolation of CSCs. The cells were isolated using our previously published method with a slight modification[18] (see Supplementary material online for further information).

2.3 EleS of CSCs

Twenty-four hours after seeding at a cell density of 3×10^5 cells/35 mm dish, the cells were serum-starved for 15 h followed by EleS (^{EleS}CSCs) using a culture cell pacer system (IonOptix). Cells were subjected to EleS for 0, 1, and 3 h at 1.5 V/1.8 cm with a biphasic square pulse (5 ms) at 5 Hz frequency. Cells without EleS ($^{Non\text{-}EleS}$CSCs) were used as baseline controls. The cells were later harvested and used for various molecular and cellular studies (see Supplementary material online for further information).

2.4 Connective tissue growth factor siRNA transfection

Ctgf-specific siRNA transfection was carried out using Lipofectamine 2000^{TM} (Invitrogen). Briefly, CSCs were transfected with 200 picomoles of *Ctgf*-specific siRNA (siCtgf). The cells transfected with scramble siRNA (siScr) (Santa Cruz Biotechnology) were used as control. After 48 h transfection with their respective siRNA, cells were harvested and used for molecular and cellular studies ($n = 4$).

2.5 Profiling of extracellular matrix and adhesion molecules

Real-time PCR-based 84 gene array RT Profiler^{TM} PCR array (SABiosciences) was used for profiling extracellular matrix (ECM) and adhesion molecules. The data thus obtained were confirmed by qRT-PCR for *Ctgf* and *Thbs-1* using specific primers (SABiosciences).

2.6 LDH and TUNEL assays

Cytoprotective effect was assessed by the CytoTox-ONE Homogeneous Membrane Integrity Assay (Promega) and by the *in situ* cell death detection kit (Roche Applied Science) per instructions of the manufacturer (see Supplementary material online for further information).

2.7 Western blot

Immunocytochemical analysis was performed as described previously[18] and as noted in *Supplementary material online, Table S1*.

2.8 RNA extraction and real-time PCR

Total RNA was isolated from various treatment groups of the cells with the RNeasy Mini kit (Qiagen), and cDNA was prepared using the Omniscript-RT kit (Qiagen). Each PCR was performed with specific primers. Real-time PCR was used to determine the expression of *Ctgf* and *Thbs1* under EleS using the QuantiTect SYBR green PCR kit (Qiagen) in a BIO-RAD-iQ5 optical module. The mRNA level was standardized to endogenous control (*Gapdh*) and expressed as fold changes.

2.9 miRNA isolation and detection

Total miRNA was extracted by the mirVanaTM miRNA Isolation kit and detected by the mirVanaTM qRT-PCR miRNA detection kit (Ambion) together with the QuantiTect SYBR green PCR kit (Qiagen) ($n = 7$). Specific miRNA primers were purchased from Ambion, and experiments were followed the instructions of the manufacturer.

2.10 Transfection with miR mimic

CSCs were transfected with miR-378 mimic (mirVana^{TM} miRNA mimic, Ambion) and Lipofectamine 2000^{TM} as described previously.[3] Briefly, CSCs were transfected with miR-378 mimic and negative control #1 (Ambion), respectively. After 48 h transfection with their mimics, cells were harvested and used for molecular and cellular studies.

2.11 Cell adhesion assay

Cell adhesion assay was performed using CytoSelect 48-well cell adhesion assay (ECM array; Cell Biolabs) per manufacturer's instruction (see Supplementary material online for further information).

2.12 Experimental model of acute myocardial infarction and cell transplantation

Myocardial infarction (MI) was carried out in mice by ligation of left anterior descending (LAD) coronary artery as described previously.[18,19] Briefly, animal surgery was performed by Drs Huang and Okada without the knowledge of any treatment. Details are given in Supplementary material online.

2.13 Immunocytochemistry

Immunocytochemical analysis was performed as described previously.[18] Briefly, CSCs were fixed in 4% paraformaldehyde, permeabilized in 1% Triton X-100 in PBS, and rinsed sequentially in PBS. Samples were incubated with specific primary antibodies, and then, with their related secondary antibodies (Supplementary material online, *Table S1*).

2.14 Statistical analysis

Results are presented as mean $\pm$ SEM. Data were evaluated statistically using one-way analysis of variance (ANOVA) followed by the Holm-Sidak method. Comparison among groups over time or groups from the same set of cells was performed by two-way repeated-measures (RM) ANOVA. Statistical significance was preset at $P < 0.05$.

3. Results

3.1 Characterization of Sca-1$^+$ CSCs

Sca-1$^+$ cells were propagated *in vitro* using the protocol as described previously (Supplementary material online, *Figure S1A*).[18] The purity of cells for Sca-1$^+$ antigen expression was determined by immunocytochemistry and flow cytometry (Supplementary material online, *Figure S1B*). To confirm the purity of CSC cultures, we performed

immunocytochemical analysis by using fibroblast markers, discoidin domain receptor 2 (DDR2), and prolyl-4-hydroxylase beta (P4HB) antibodies.[20] Rarely, CSC cultures were DDR2 and P4HB positive (Supplementary material online, *Figure S1C*). Fluorescence activated cell sorting analysis also showed that isolated CSC cultures maintained ~80–90% of Sca-1$^+$ cells from passages 5–30 (Supplementary material online, *Figure S1B*). These cells showed significantly high expression of pluripotency markers including *Nanog* as well as *Bcrp1* (stem-rich side population)[21] and were also positive for early cardiac transcription factors such as GATA4, Nkx2.5, and MEF2c (Supplementary material online, *Figure S1D*).[18,22]

3.2 EleS improves CSC survival *in vitro* against oxidative stress

IPC has been well studied *in vitro* and *in vivo*. It provides early cytoprotective effect for 4 h and late cytoprotection from 24 to 48 h later, which is known as the second window of protection.[23,24] To investigate the cytoprotective effects of EleS, we subjected CSCs to EleS and IPC and kept these cells in the normal medium for 0, 5, 8, and 24 h, and then, treated with H_2O_2 for 5 h and performed LDH assay using IPC as a positive control (Supplementary material online, *Figure S2A*). As expected, EleS reduced cytotoxicity in CSCs until 5 h of H_2O_2 treatment as examined by LDH assay (*Figure 1A*). Similarly, ^{EleS}CSCs showed significantly a lower number of TUNEL-positive cells (5.85 ± 1.27%) when compared with the $^{Non\text{-}EleS}$CSC group (15.03 ± 2.59%) (*Figure 1B*). Phase contrast microscopy showed rounded and hyper-contracted morphology of $^{Non\text{-}EleS}$CSCs while ^{EleS}CSCs indicated well-preserved morphology (*Figure 1C*). However, the second window of cytoprotection by EleS after 24 h was not observed (*Figure 1A*).

3.3 AKT is involved in EleS-induced CSC survival

Next, we sought to determine the underlying mechanism involved in pro-survival effects of EleS. EleS-induced protein expressions on CSCs

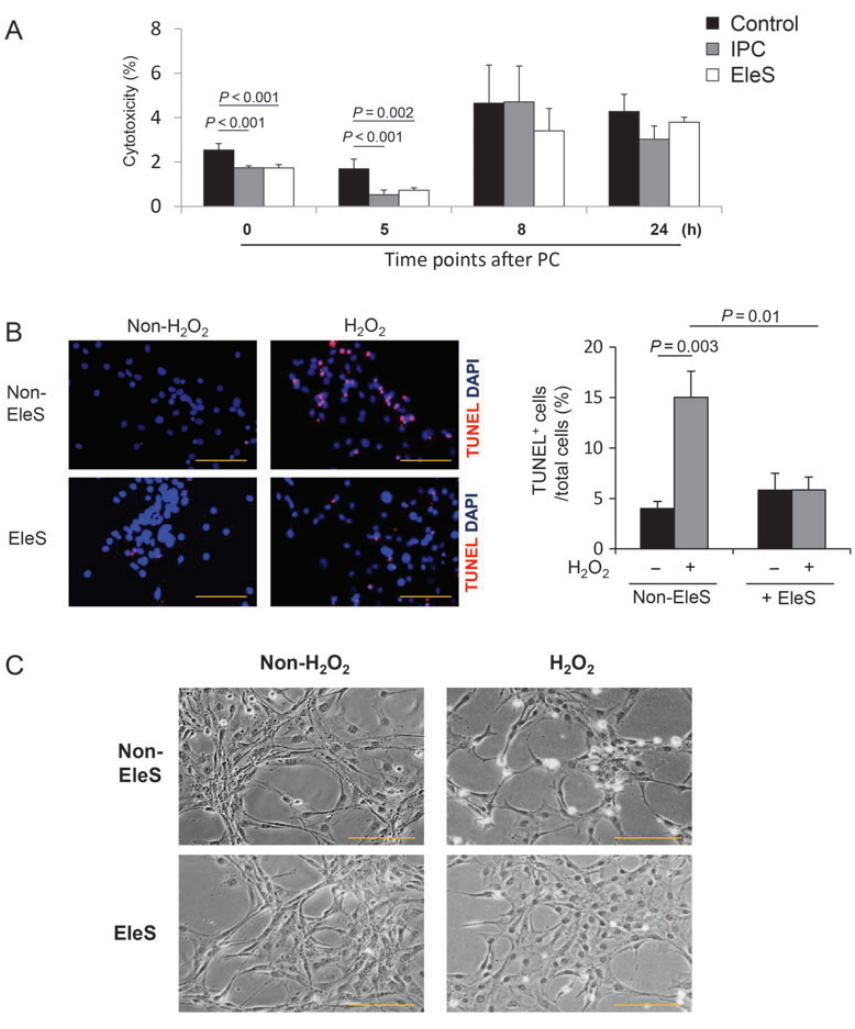

Figure 1 Effects of EleS on cytoprotection of CSCs. (*A*) Three groups (control, EleS, and IPC) were treated with H_2O_2 for 5 h at 0, 5, 8, and 24 h later after EleS and IPC. EleS reduced cell injury (LDH release) for 5 h, but had no effect after 8–24 h, while IPC exhibited the second window of protection after 24 h ($n = 4$). (*B*) Representative fluorescence images and quantitative analysis of TUNEL positivity in ^{EleS}CSCs (red = TUNEL-positive nuclei; blue = DAPI) ($n = 5$). (*C*) Morphological changes in CSCs treated with H_2O_2. Phase contrast images showed that $^{Non\text{-}EleS}$CSCs were rounded-off and shrunk and EleS prevented these morphological changes. 3×10^5 cells/35 mm dish. Data were analysed by two-way RM ANOVA. Bar = 100 μm.

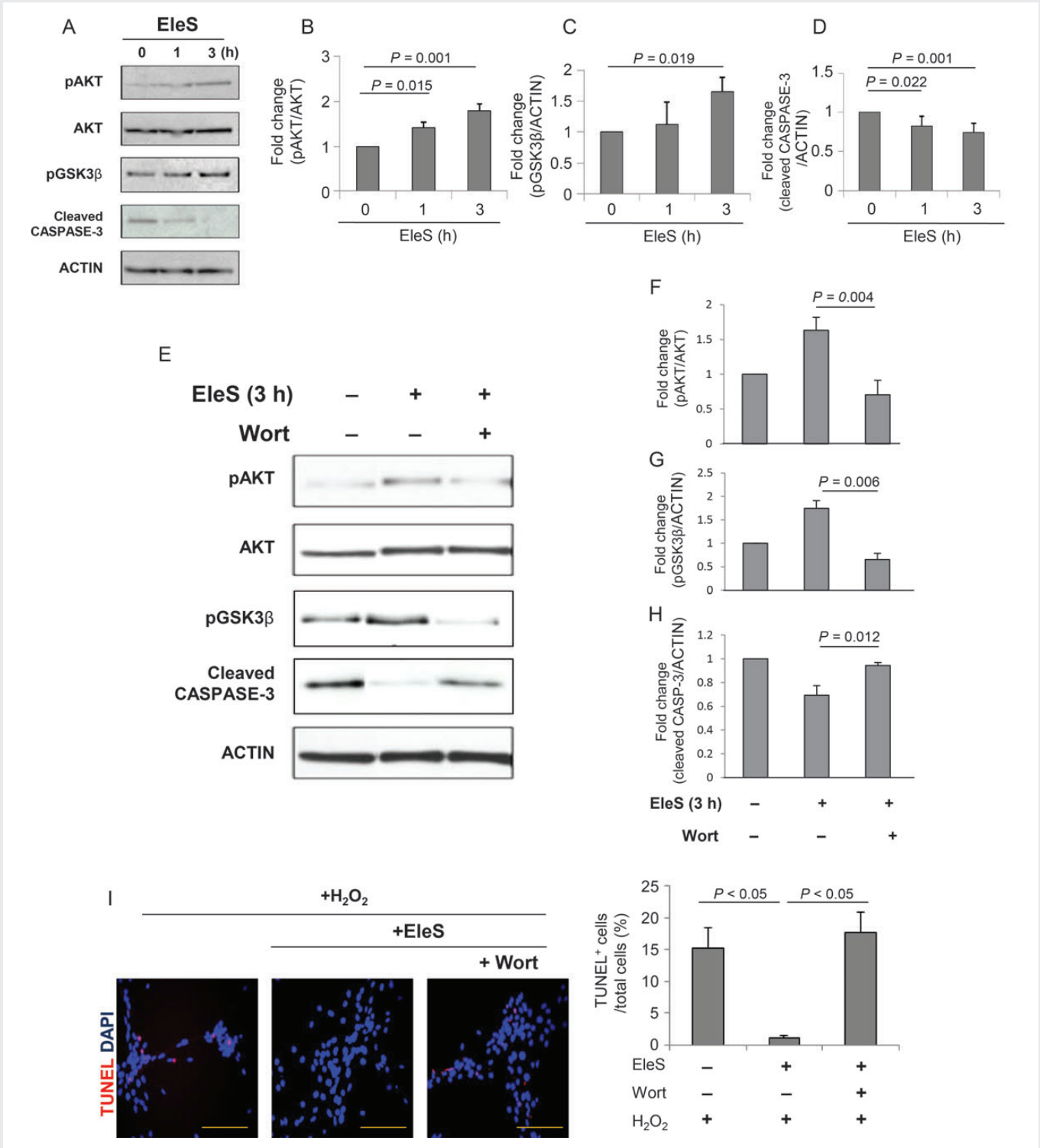

Figure 2 Involvement of the AKT signalling pathway in EleS-induced CSC survival. (*A–D*) EleS-induced protein expression in CSCs were measured by Western blot in a time-dependent manner. A significantly higher phosphorylation of AKT and less cleavage of caspase-3 were showed in ^{EleS}CSCs when compared with $^{Non\text{-}EleS}$CSCs in a time-dependent manner. Total AKT expression remained unchanged in ^{EleS}CSCs ($n = 4$). (*E–H*) Increase in p-AKT and p-GSK3β and decrease in cleaved caspase-3 induced by EleS were abolished by Wortmannin treatment ($n = 4$). One-way RM ANOVA. (*I*) Pre-treatment with Wortmannin significantly reduced cell survival as determined by TUNEL assay ($n = 5$). 3×10^5 cells/35 mm dish. One-way ANOVA (Dunn's method). Bar = 100 μm.

were examined at 0, 1, and 3 h of EleS by western blot. *Figure 2A* and *B* showed a significant increase in activation of AKT in ^{EleS}CSCs when compared with $^{Non\text{-}EleS}$CSCs ($P = 0.001$), whereas total AKT expression was not altered. EleS also induced significantly higher phosphorylation of GSK3β ($P = 0.019$, *Figure 2A* and *C*) and reduced caspase-3 cleavage ($P = 0.001$, *Figure 2A* and *D*). Pre-treatment of ^{EleS}CSCs with 5 μM Wortmannin for 30 min abolished AKT phosphorylation as well as downstream signalling molecules such as GSK3β and caspase-3 cleavage. ^{EleS}CSCs increased phosphorylation of AKT and GSK3β time-dependently (*Figure 2A–C*), whereas the expression of cleaved caspase-3 gradually decreased (*Figure 2A* and *D*). However, Wortmannin abolished EleS-induced increases in phosphorylation of AKT and GSK3β (*Figure 2E–G*) and decrease in cleaved caspase-3 (*Figure 2E* and *H*). Furthermore, TUNEL-positive cell death was increased in ^{EleS}CSCs when treated with Wortmannin (*Figure 2I*).

3.4 EleS induces FAK activation for cell adhesion and survival

While studying the anti-apoptotic effects of EleS via activation of AKT under oxidative stress, we observed that number of the cells attached to culture dish was obviously higher in ^{EleS}CSCs when compared with $^{Non\text{-}EleS}$CSCs. This observation was confirmed by colorimetric cell adhesion assay with crystal violet (*Figure 3A*) as well as fluorescence signals (*Figure 3B*). The pro-adherent effects of EleS were abrogated by pre-treatment of ^{EleS}CSCs with Wortmannin when compared with dimethyl sulfoxide (solvent for the inhibitors)-treated ^{EleS}CSCs (*Figure 3A* and *B*). To determine the role of FAK that plays a critical role in cell adhesion,[25] CSCs were pre-treated with 25 μM FI-14, a FAK inhibitor. FI-14 treatment of CSCs, either in the presence or absence of EleS, significantly reduced cell adhesion upon subsequent treatment with H_2O_2 as determined by both colorimetric and fluorometric cell adhesion assays (*Figure 3A* and *B*, Supplementary material online, *Figure S3*). Western blot showed significantly higher phosphorylation of FAK (p-FAK, at Y397) in a time-dependent manner, whereas total FAK expression in ^{EleS}CSCs was not altered during PC with EleS (*Figure 3C*). TUNEL assay showed that pre-treatment with FI-14 abolished the PC effect of EleS (*Figure 3D*). Pre-treatment of FI-14 markedly inhibited phosphorylation of both FAK and AKT, whereas Wortmannin treatment only inhibited p-AKT, but not p-FAK in ^{EleS}CSCs (*Figure 3E–G*), thus suggesting that FAK, an upstream molecule of AKT, plays an important role in cell adhesion induced by EleS.

3.5 CTGF is a critical regulator of cell adhesion induced by EleS

Since ECM and cell adhesion molecules play an important role in cell survival, we performed real-time PCR-based array to search for responsible factors for ECM and cell adhesion induced by EleS (*Figure 4A*). The candidate genes were selected from the most up-regulated and down-regulated genes. *Thbs-1* and *Ctgf* were up-regulated by 2.35- and 1.9-folds, whereas *Mmp13*, *Mmp11* and *Col3a1* were down-regulated by 2.79-, 1.87-, and 1.87-folds, respectively. Because CTGF is a well-known growth factor involved in cell survival, tissue repair, and angiogenesis,[26,27] we selected *Ctgf* as a potential candidate responsible for EleS-induced cell adhesion and survival. The mRNA and protein expression of *Ctgf* was validated with RT-PCR and western blot (*Figure 4B* and *C*). Immunocytochemical analysis also showed that ^{EleS}CSCs were positive for CTGF (87.44 ± 4.08%) when compared with $^{Non\text{-}EleS}$CSCs (27.51 ± 7.82%) (*Figure 4D*).

To investigate the role of CTGF in ^{EleS}CSC survival and adhesion, CTGF was abrogated in ^{EleS}CSCs by siCtgf (*Figure 4E*). At 48 h after respective transfection of siRNA, ∼50% of successful abrogation of CTGF was confirmed when compared with the siScr-transfected ^{EleS}CSCs, as examined by western blot (*Figure 4E*). siCtgf-transfected ^{EleS}CSCs showed significantly higher percentage of TUNEL-positive cell death when compared with siScr-transfected ^{EleS}CSCs (*Figure 4F*). Interestingly, cell adhesion assay showed that CTGF abrogation significantly reduced the number of adhering cells subsequent to H_2O_2 treatment (*Figure 4G* and *H*). Western blot analysis showed that EleS-induced CTGF expression was abolished by pre-treatment with Wortmannin and FI-14 (*Figure 4I* and *J*), indicating that CTGF induced by EleS enhances CSC adhesion and survival through FAK and AKT pathways.

3.6 Transplantation of ^{EleS}CSCs restores ischaemic heart function

To investigate the cell survival and functional role of ^{EleS}CSC in ischaemic heart *in vivo*, CSCs with or without EleS were transplanted into the infarcted heart using the mouse LAD ligation model. Real-time PCR for *Sry* gene in the infarcted heart on Day 4 demonstrated higher survival of the transplanted cells pre-conditioned by EleS. As expected, *Sry* gene expression was increased in the ^{EleS}CSC-transplanted group, when compared with the $^{Non\text{-}EleS}$CSC group (*Figure 5A*). Similarly, we observed a higher number of Q-dot nanocrystal-labelled ^{EleS}CSCs in the infarcted heart when compared with that of the $^{Non\text{-}EleS}$CSC group (*Figure 5B*). The indices of left ventricle (LV) contractile function were well preserved in the ^{EleS}CSC group after 4 weeks with an ejection fraction (LVEF) of 43.94 ± 2.91% compared the control group (24.56 ± 2.61%) and $^{Non\text{-}EleS}$CSC group (31.55 ± 1.78%). Similarly, fractional shortening (FS) though was improved but not statistically significant from the $^{Non\text{-}EleS}$CSC group at 4 weeks. LVFS in the ^{EleS}CSC group was also improved at 4 weeks of transplantation (21.15 ± 1.24%) when compared with the control group and $^{Non\text{-}EleS}$CSC group (11.63 ± 1.27 and 16.98 ± 1.95%, respectively) (*Figure 5C*). The left ventricular end-diastolic volume (LVEDV) in the ^{EleS}CSC group at 4 weeks (73.29 ± 9.12 mm^3) was reduced when compared with the control group (125.14 ± 13.87 mm^3). The left ventricular end-systolic volume (LVESV) was significantly reduced to 42.17 ± 6.12 mm^3 in the ^{EleS}CSC group at 4 weeks compared with the control group (93.44 ± 8.49 mm^3), suggesting better contractile function in ^{EleS}CSC-transplanted animals (*Figure 5D*).

Furthermore, transplantation of ^{EleS}CSCs transfected with specific siRNA for Ctgf abolished the effect of EleS, suggesting that CTGF is responsible for EleS-induced CSC survival (*Figure 5E*). In addition, the limited number of Q-dot nanocrystal-labelled cells were found in the siCtgf-transfected CSC group ($n = 5$) than in the siScr-CSC group ($n = 4$) (*Figure 5F*). Moreover, inhibition of Ctgf in ^{EleS}CSCs abrogated the EleS-induced improvement of cardiac functional indices (*Figure 5G* and *H*). Taken together, these results indicate that EleS promotes CSC survival and functional recovery of the infarcted heart through Ctgf up-regulation.

3.7 miR-378 regulates CTGF expression and cell survival signalling in EleS pre-conditioning

To investigate the involvement of miRNAs responsible for *Ctgf* regulation, miRNA microarray was carried out and candidate miRNAs were selected based on fold changes (Supplementary material online, *Table S2*).

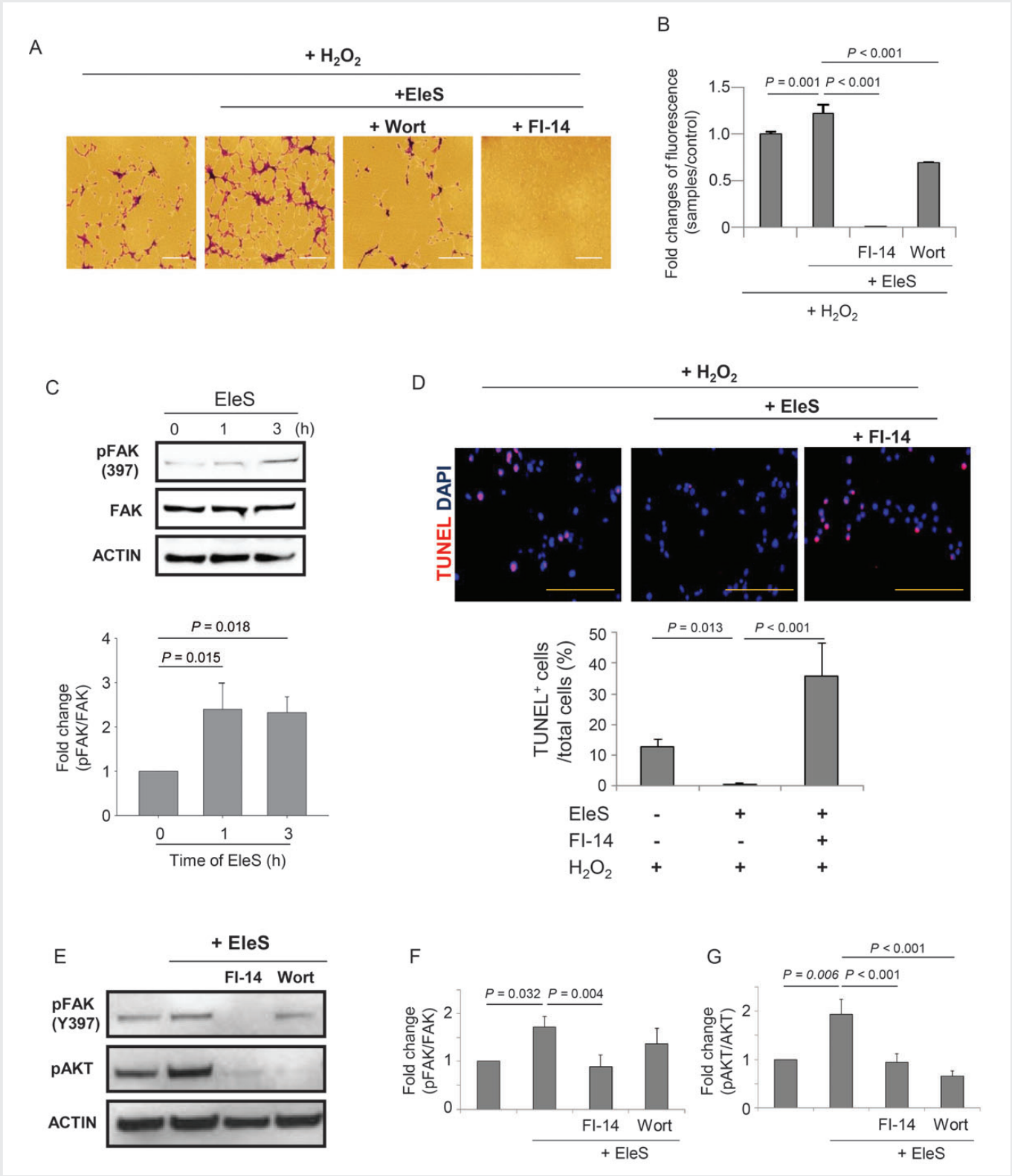

Figure 3 EleS stimulates CSC adhesion and survival via FAK phosphorylation. (*A* and *B*) Cell adhesion was enhanced by EleS and inhibited by Wortmannin and FI-14. (*C*) EleS showed significant up-regulation of phosphorylated FAK at Tyr-397 as examined by western blot. Phosphorylation of FAK was increased in a time-dependent manner. (*D*) The number of TUNEL-positive cells in ^{EleS}CSCs was significantly increased by pre-treatment with FI-14. Bar = 100 μm. (*E*–*G*) Pre-treatment with FI-14 significantly abolished phosphorylation of FAK and AKT, whereas pre-treatment with Wortmannin abolished only phosphorylation of AKT, but not FAK in ^{EleS}CSCs ($n = 5$). 3×10^5 cells/35 mm dish. Data were analysed by one-way RM ANOVA.

A

	Up-regulation
Thbs1	2.35
Ctgf	1.90
Adamts2	1.35
Sgce	1.31

	Down-regulation
Mmp15	−1.42
Col3a1	−1.87
Mmp11	−1.87
Mmp13	−2.79

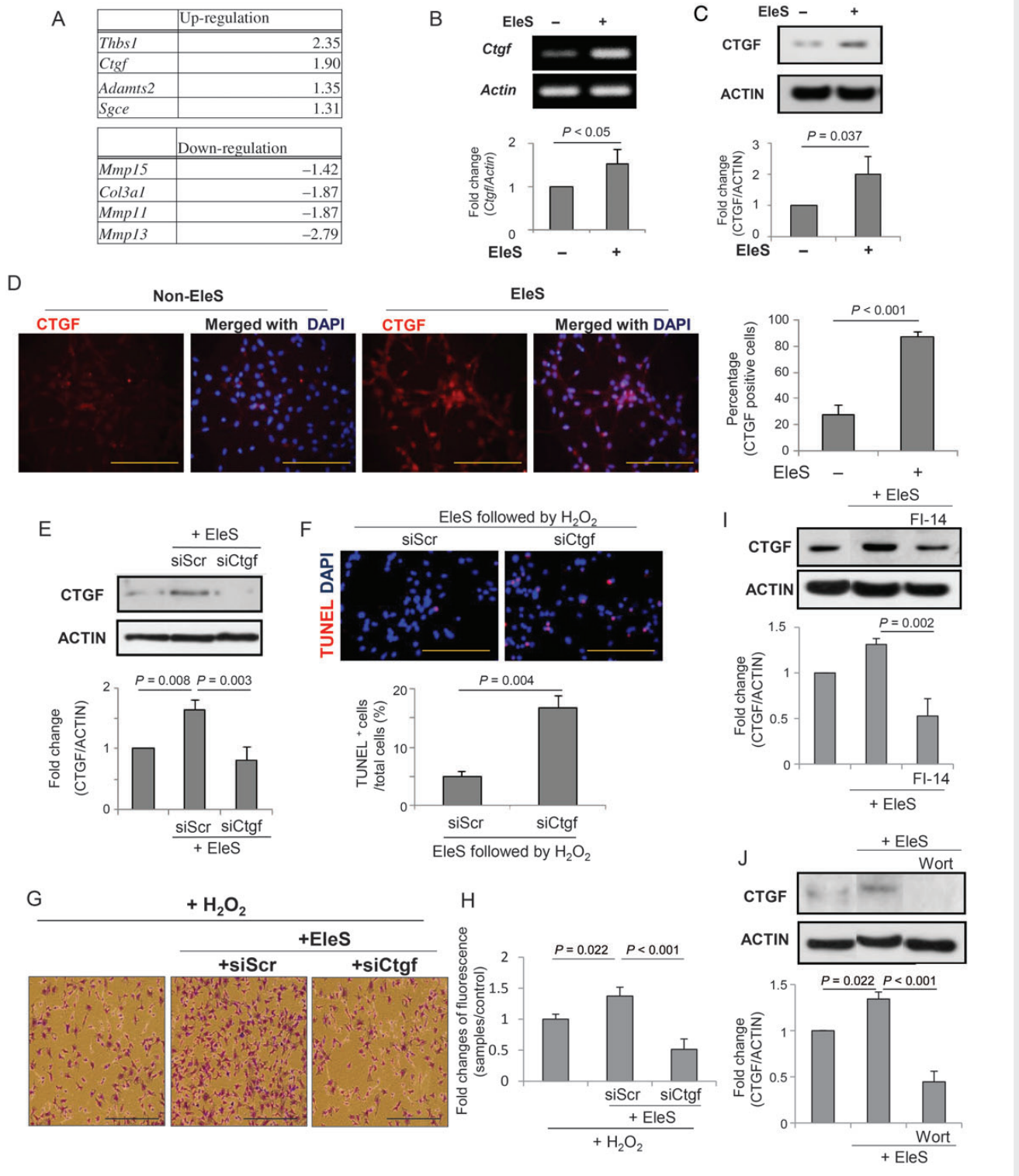

Figure 4 CTGF is a major downstream factor for EleS-induced FAK/AKT pathways. (*A*) Real-time PCR-based gene expression profiling was performed for ECM and cell adhesion molecules. Four of each up-regulated and down-regulated genes were selected based on fold change. (*B* and *C*) mRNA expression of *Ctgf* was confirmed by conventional RT–PCR and real-time PCR ($n = 5$). Paired *t*-test. (*D*) CTGF positivity by immunocytochemistry was higher in ^{EleS}CSCs when compared with $^{Non\text{-}EleS}$CSCs. (*E*) EleS-induced CTGF protein expression was inhibited by siCtgf transfection. (*F*) Knockdown of CTGF by specific siRNA increased TUNEL$^+$ apoptotic cell death. (*G* and *H*) Cell adhesion induced by EleS was decreased by inhibiting CTGF by siRNA and confirmed by crystal violet staining ($n = 3$) and fluorescence cell adhesion assay ($n = 6$). (*I* and *J*) Western blot showed that overexpression of CTGF induced by EleS was decreased when treated with FI-14 and Wortmannin. 3×10^5 cells/35 mm dish. Data were analysed by one-way RM ANOVA. Bar = 100 μm.

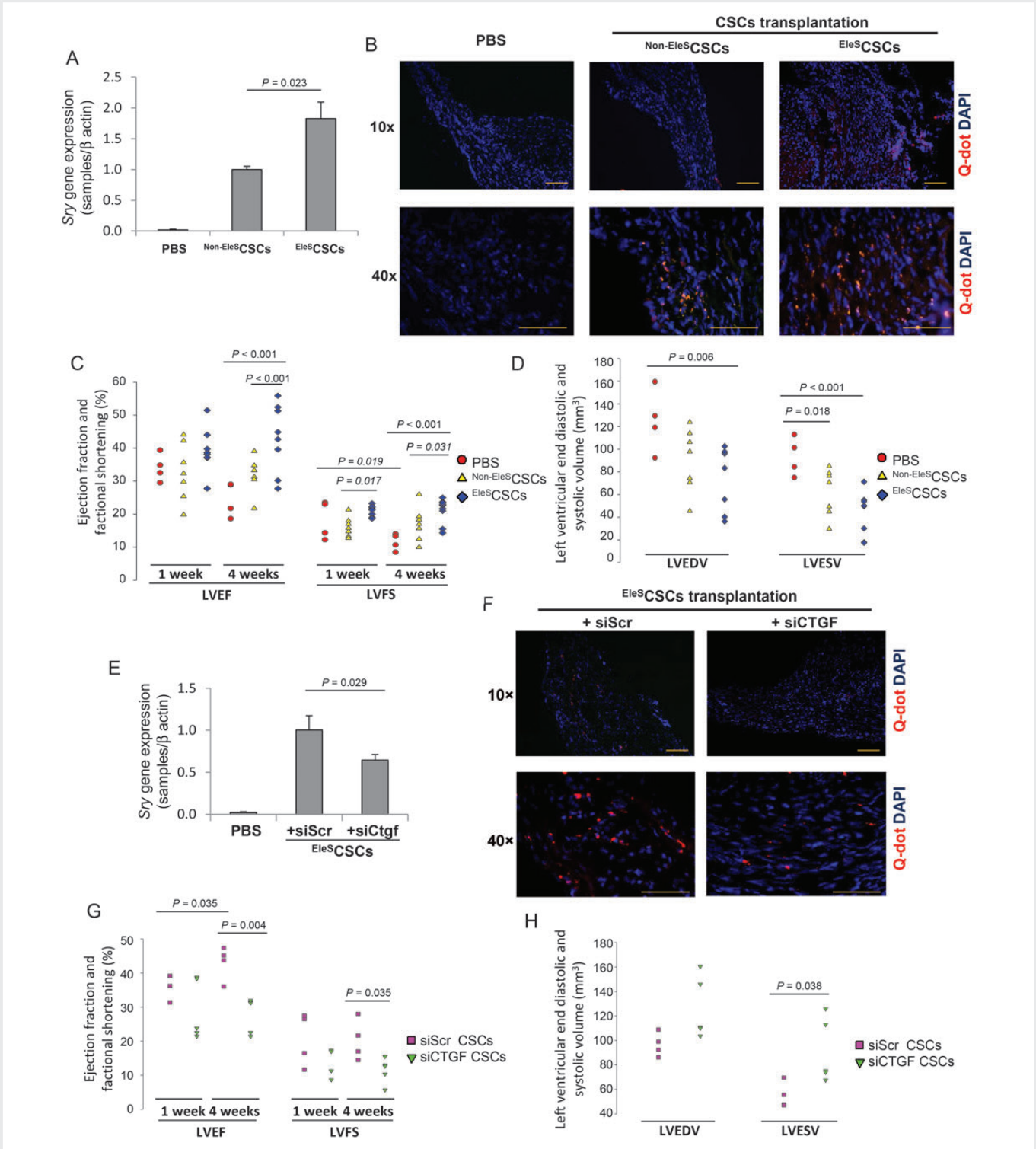

Figure 5 Transplantation of ^{EleS}CSCs restores cardiac function after MI. (*A*) *Sry* gene expression was 1.83-fold higher in hearts transplanted with ^{EleS}CSCs when compared with $^{Non\text{-}EleS}$CSCs ($n = 4$, Student's *t*-test). (*B*) Heart samples were prepared 4 weeks after cell transplantation. Transplanted Q-dot nanocrystal-labelled $^{Non\text{-}EleS}$CSCs and ^{EleS}CSCs (red) were detected in infarcted and peri-infarcted area (blue = DAPI). (*C*) LVEF and LVFS were calculated in ^{EleS}CSCs ($n = 9$) vs. control ($n = 4$) and $^{Non\text{-}EleS}$CSCs ($n = 7$) in 1 and 4 weeks (analysed by two-way RM ANOVA). (*D*) Cavity size measured by LVESV was significantly reduced at 4 weeks after ^{EleS}CSCs transplantation compared with control and appeared to be smaller in hearts than those transplanted with $^{Non\text{-}EleS}$CSCs (analysed by one-way ANOVA). (*E*) Higher *Sry* gene expression in the ^{EleS}CSCs transplanted group was abolished by siCtgf transfection in *in vivo* murine ischaemic heart ($n = 5$, Student's *t*-test). (*F*) Transplantation of ^{EleS}CSCs transfected with specific siRNA for Ctgf abolished the effect of EleS (blue = DAPI). (*G* and *H*) siCtgf did not restore cardiac function by EleS (LVEF and LVFS analysed by two-way RM ANOVA; LVEDV and LVESV by Student's *t*-test). Bar = 100 μm.

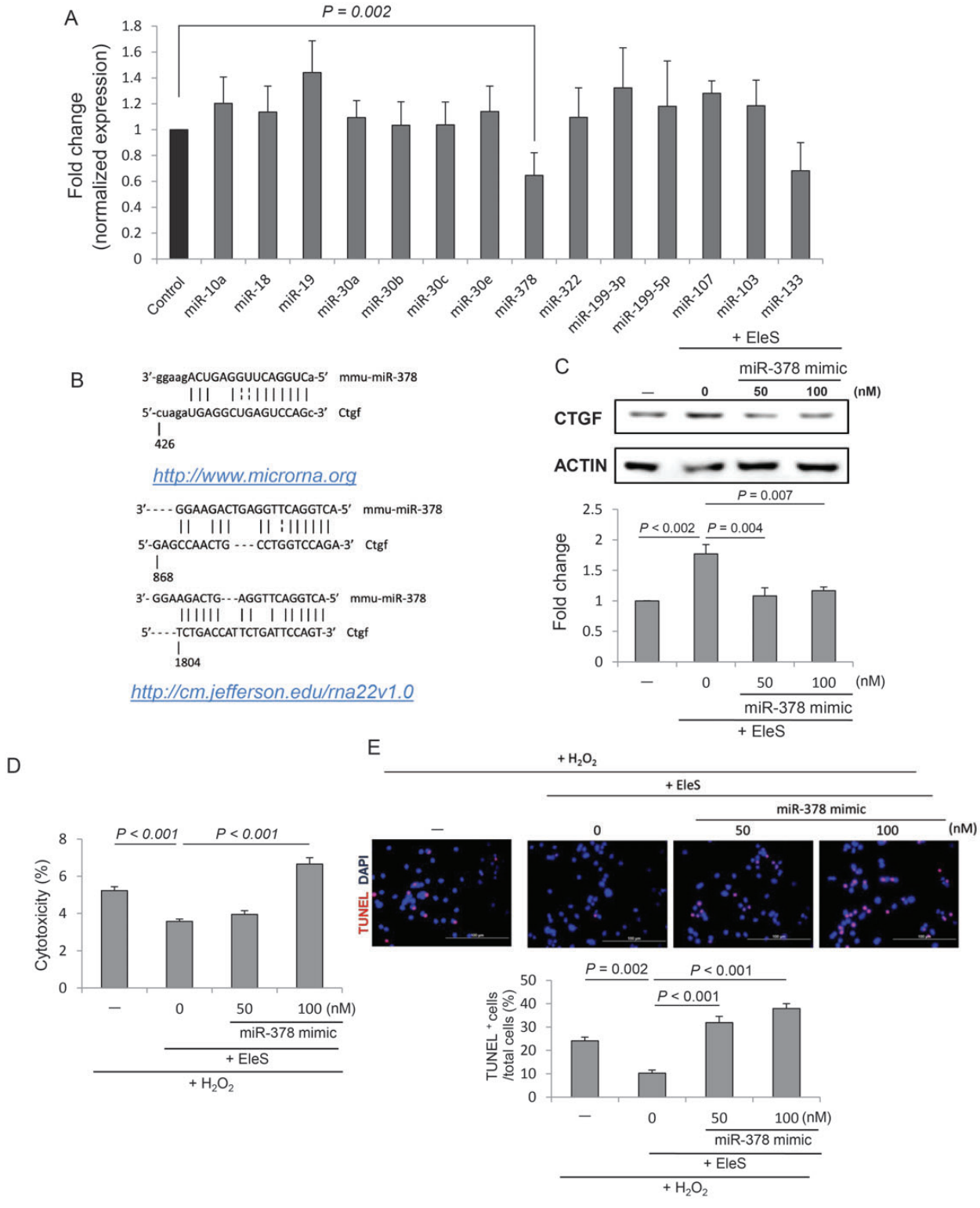

Figure 6 miR-378 regulates Ctgf expression and cell survival signalling in EleS PC. (*A*) miRNA profiling in ^{EleS}CSCs by miR microarray and real-time PCR. miRNA expression in ^{EleS}CSCs was normalized with those in $^{Non\text{-}EleS}$CSCs. miR-378 expression was significantly down-regulated in ^{EleS}CSCs ($n = 6$). (*B*) Three putative 3′-UTR sites in *Ctgf* for miR-378 binding predicted by two computational analysis programmes (http://www.microrna.org; http://cm.jefferson.edu/rna22v1.0). (*C*) Overexpression of miR-378 by mimic transfection in ^{EleS}CSCs inhibited CTGF expression. ACTIN was used as a loading control ($n = 3$). (*D*) Overexpression of miR-378 mimic abrogated EleS-induced cytoprotective effect in CSCs against H_2O_2-induced oxidative stress. (*E*) The number of TUNEL-positive cells was increased by transfection of ^{EleS}CSCs with miR-378 mimic ($n = 3$). Data were analysed by one-way RM ANOVA. Scale bar = 100 μm.

By using the computational analysis programme (http://www.mirnabodymap.org),[28] 14 candidate miRNAs were chosen and validated by real-time PCR (*Figure 6A*). Target prediction tools (http://www.microrna.org/[29] and http://cm.jefferson.edu/rna22v1.0/)[30] identified three sets of matches of a mmu-miR-378 sequence along with the flanking nucleotides within the 3′-untranslated region (UTR) of *Ctgf* (*Figure 6B*). To validate these predictions, miR-378 were overexpressed by miR-378 mimic transfection (50 and 100 nM), and overexpression of miR-378 resulted in inhibition of CTGF protein expression (*Figure 6C*), suggesting that miR-378 targets CTGF. To examine the effect of miR-378 overexpression on cell survival, we performed miR-378 mimic transfection of ^{EleS}CSCs. As expected, overexpression of miR-378 abolished EleS-induced cytoprotective effects in CSCs as examined by LDH and TUNEL assays (*Figure 6D* and *E*). These results suggest that miR-378 is a key determinant for CSC survival induced by EleS PC.

4. Discussion

This study demonstrates that (i) stem cells subjected to EleS are strongly protected against oxidant/ischaemia-induced lethal injury and promote functional recovery of the ischaemic heart, (ii) the endogenous protection as a result of EleS is initiated by FAK/AKT activation resulting in the release of CTGF, supporting firm cell adhesion and attenuation of cell apoptosis, (iii) CTGF expression by EleS was regulated by miR-378. Several studies reported differentiation effect induced by EleS in mesenchymal stem cells[12] and embryonic stem cells.[13,14] However, cytoprotective effects of EleS in stem cells have not been studied.

The effect of PC by EleS is different from that of typical IPC. Both have a cytoprotective effect on cells in common. In the present study, EleS did not show the statistically significant effect of the second window of protection, which is shown to be due to *de novo* protein synthesis by IPC after 24 h.[23,24] Additionally, the protection/survival mechanisms may involve different pathways between cell culture and intact organs. Although we did not study the direct effect of EleS in the intact hearts that may relate to diverse signalling molecules, the isolated cells may likely participate in pathways parallel to intact organs.

Longer survival of CSC *in vivo* conditions over 4 weeks is at variance with *in vitro* data showing protection only for 5 h. Shorter cytoprotective effects of EleS in *in vitro* condition may be due to cell culture conditions or extreme oxidative stress in this study. *In vitro* cell culture conditions are much different from *in vivo* cardiac microenvironment, which includes repeated electrical and mechanical stimulation by the heart or less harsh environment. H_2O_2 concentration we used in this study to induce apoptosis is quite different from *in vivo* environment. Even short-time adaptation of CSCs to EleS showed a higher survival rate in *in vitro* oxidative stress as well as *in vivo* infarcted heart. The other important factor we propose is paracrine activity of EleS-mediated CSCs. Paracrine factors released from EleS-mediated CSCs would support repair of injured cardiomyocytes as well as differentiation of CSCs, which can restore functional recovery of ischaemic heart. Additional studies will likely shed light in the factors described.

Focal adhesion of cells stimulates FAK, the phosphorylation of which at Y397 activates PI3K/AKT important in cell adhesion and survival in anchorage-dependent cells.[31–33] Detachment from surrounding ECM initiates a special type of apoptosis, so-called 'anoikis'. Cell adhesion phosphorylates FAK through integrin and receptor tyrosine kinase and allows the cell to communicate with surrounding ECM for survival signalling, preventing anoikis. Phosphorylated FAK at Y397 by integrin and receptor tyrosine kinase recruits SH2 domain protein including PI3K, phospholipase C, and adaptor Grb7 to the linker region.[32] Nuclear translocation of FAK promotes cell survival and proliferation via p53 activities.[34] Also, a recent study in human Schwannoma cells shows that insulin-like growth factor-binding protein increases cell survival and proliferation by both phosphorylation and nuclear translocation of FAK and activation of AKT.[35]

CTGF was markedly expressed in ^{EleS}CSCs, implying that it may play an important role in EleS-induced cell survival and adhesion and functions as an autocrine growth factor. CTGF is known to exert its effect on tissue repair, scarring, fibrosis,[36] cytoprotection against ischaemic reperfusion injury,[37] and endothelial cell adhesion and survival.[38] CTGF is also known to bind with transforming growth factor-β, extracellular matrix, integrin, and bone morphogenetic protein (BMP4), thus stimulating diverse cellular pathways.[39] The previous studies reported that up-regulation of CTGF is mediated through FAK/AKT pathways.[40,41] These conclusions are well supported by our data. However, CTGF expression in this study was independent of TGFβ involvement (data not shown). Therefore, additional studies are needed to elucidate the role of CTGF in EleS-mediated protection.

Interestingly, we found that miR-378 regulated EleS-induced CTGF expression. Several miRNAs have been reported to target CTGF. In aged heart, decreased miR-18 and miR-19 increased CTGF and thrombospondin-1 expression.[42] Another report showed that both miR-133 and miR-30 regulate CTGF, implying myocardial matrix remodelling.[43] This is the first report that miR-378 targets CTGF. Interestingly, a recent study showed that down-regulation of miR-378 supports cell survival by targeting insulin-like growth factor 1 receptor (IGF-1R) in cardiomyocytes and acts as a negative regulator.[44] In the later study, IGF-1/IGF-1R system triggers cell survival signals, via the p-AKT signalling pathway, and reduces levels of apoptosis inducing factors, Bim, Tranil, and FasL. In spite of another report that overexpression of miR-378 enhanced cell survival by targeting caspase-3, our finding showed down-regulation of both caspase-3 and miR-378 under EleS. It is also likely that cytoprotective effects of EleS may be mediated with other pathways or different cell types may react differently by EleS. Further studies are needed to understand the mechanism of EleS-induced miRNAs.

In conclusion, EleS of stem cells is a powerful novel technique to take advantage of cellular endogenous mechanism for stem cell survival against ischaemic insult and to restore the cardiac function after MI. Ctgf via FAK/AKT signalling plays a pivotal role in EleS-mediated protection of stem cells.

Supplementary material

Supplementary material is available at *Cardiovascular Research* online.

Acknowledgements

We thank Dr Michitaka Takamiya, a fellow in Dr Ashraf laboratory, for scientific advice for isolation of Sca-1$^+$ CSCs. We are thankful to Dr Jeffrey Welge for his assistance in statistical analyses and he was supported by the National Center for Research Resources and the National Center for Advancing Translational Sciences, National Institutes of Health, through Grant 8 UL1 TR000077-05.

Conflict of interest: none declared.

Funding

This work was supported by National Institutes of Health grants (HL087246; R37 HL 074272; to M.A.).

References

1. Niagara MI, Haider HK, Jiang S, Ashraf M. Pharmacologically preconditioned skeletal myoblasts are resistant to oxidative stress and promote angiomyogenesis via release of paracrine factors in the infarcted heart. *Circ Res* 2007;**100**:545–555.
2. Hoke NN, Salloum FN, Kass DA, Das A, Kukreja RC. Preconditioning by phosphodiesterase-5 inhibition improves therapeutic efficacy of adipose-derived stem cells following myocardial infarction in mice. *Stem Cells* 2012;**30**:326–335.
3. Kim HW, Haider HK, Jiang S, Ashraf M. Ischemic preconditioning augments survival of stem cells via miR-210 expression by targeting caspase-8-associated protein 2. *J Biol Chem* 2009;**284**:33161–33168.
4. Rajapakse N, Kis B, Horiguchi T, Snipes J, Busija D. Diazoxide pretreatment induces delayed preconditioning in astrocytes against oxygen glucose deprivation and hydrogen peroxide-induced toxicity. *J Neurosci Res* 2003;**73**:206–214.
5. Yau TM, Kim C, Ng D, Li G, Zhang Y, Weisel RD *et al*. Increasing transplanted cell survival with cell-based angiogenic gene therapy. *Ann Thorac Surg* 2005;**80**:1779–1786.
6. Mangi AA, Noiseux N, Kong D, He H, Rezvani M, Ingwall JS *et al*. Mesenchymal stem cells modified with Akt prevent remodeling and restore performance of infarcted hearts. *Nat Med* 2003;**9**:1195–1201.
7. Hutter JJ, Mestril R, Tam EK, Sievers RE, Dillmann WH, Wolfe CL. Overexpression of heat shock protein 72 in transgenic mice decreases infarct size in vivo. *Circulation* 1996;**94**:1408–1411.
8. Wang X, Zhao T, Huang W, Wang T, Qian J, Xu M *et al*. Hsp20-engineered mesenchymal stem cells are resistant to oxidative stress via enhanced activation of Akt and increased secretion of growth factors. *Stem Cells* 2009;**27**:3021–3031.
9. Dubey AK, Gupta SD, Basu B. Optimization of electrical stimulation parameters for enhanced cell proliferation on biomaterial surfaces. *J Biomed Mater Res B Appl Biomater* 2011;**98**:18–29.
10. Chang KA, Kim JW, Kim JA, Lee SE, Kim S, Suh WH *et al*. Biphasic electrical currents stimulation promotes both proliferation and differentiation of fetal neural stem cells. *PLoS One* 2011;**6**:e18738.
11. McCaig CD, Rajnicek AM, Song B, Zhao M. Controlling cell behavior electrically: current views and future potential. *Physiol Rev* 2005;**85**:943–978.
12. Genovese JA, Spadaccio C, Chachques E, Schussler O, Carpentier A, Chachques JC *et al*. Cardiac pre-differentiation of human mesenchymal stem cells by electrostimulation. *Front Biosci* 2009;**14**:2996–3002.
13. Sauer H, Rahimi G, Hescheler J, Wartenberg M. Effects of electrical fields on cardiomyocyte differentiation of embryonic stem cells. *J Cell Biochem* 1999;**75**:710–723.
14. Chen MQ, Xie X, Hollis Whittington R, Kovacs GT, Wu JC, Giovangrandi L. Cardiac differentiation of embryonic stem cells with point-source electrical stimulation. *Conf Proc IEEE Eng Med Biol Soc* 2008;**2008**:1729–1732.
15. Serena E, Figallo E, Tandon N, Cannizzaro C, Gerecht S, Elvassore N *et al*. Electrical stimulation of human embryonic stem cells: cardiac differentiation and the generation of reactive oxygen species. *Exp Cell Res* 2009;**315**:3611–3619.
16. Baba T, Kameda M, Yasuhara T, Morimoto T, Kondo A, Shingo T *et al*. Electrical stimulation of the cerebral cortex exerts antiapoptotic, angiogenic, and anti-inflammatory effects in ischemic stroke rats through phosphoinositide 3-kinase/Akt signaling pathway. *Stroke* 2009;**40**:e598–e605.
17. Zhao M, Bai H, Wang E, Forrester JV, McCaig CD. Electrical stimulation directly induces pre-angiogenic responses in vascular endothelial cells by signaling through VEGF receptors. *J Cell Sci* 2004;**117**:397–405.
18. Takamiya M, Haider KH, Ashraf M. Identification and characterization of a novel multipotent sub-population of Sca-1^{+} cardiac progenitor cells for myocardial regeneration. *PLoS One* 2011;**6**:e25265.
19. Tarnavski O, McMullen JR, Schinke M, Nie Q, Kong S, Izumo S. Mouse cardiac surgery: comprehensive techniques for the generation of mouse models of human diseases and their application for genomic studies. *Physiol Genomics* 2004;**16**:349–360.
20. Skoumal R, Tóth M, Serpi R, Rysä J, Leskinen H, Ulvila J *et al*. Parthenolide inhibits STAT3 signaling and attenuates angiotensin II-induced left ventricular hypertrophy via modulation of fibroblast activity. *J Mol Cell Cardiol* 2011;**50**:634–641.
21. Zhou S, Schuetz JD, Bunting KD, Colapietro AM, Sampath J, Morris JJ *et al*. The ABC transporter Bcrp1/ABCG2 is expressed in a wide variety of stem cells and is a molecular determinant of the side-population phenotype. *Nat Med* 2001;**7**:1028–1034.
22. Beltrami AP, Barlucchi L, Torella D, Baker M, Limana F, Chimenti S *et al*. Adult cardiac stem cells are multipotent and support myocardial regeneration. *Cell* 2003;**114**:763–776.
23. Zhou X, Zhai X, Ashraf M. Direct evidence that initial oxidative stress triggered by preconditioning contributes to second window of protection by endogenous antioxidant enzyme in myocytes. *Circulation* 1996;**93**:1177–1184.
24. Hausenloy DJ, Yellon DM. The second window of preconditioning (SWOP) where are we now? *Cardiovasc Drugs Ther* 2010;**24**:235–254.
25. Frame MC, Patel H, Serrels B, Lietha D, Eck MJ. The FERM domain: organizing the structure and function of FAK. *Nat Rev Mol Cell Biol* 2010;**11**:802–814.
26. Shi-wen X, Stanton LA, Kennedy L, Pala D, Chen Y, Howat SL *et al*. CCN2 Is necessary for adhesive responses to transforming growth factor-beta1 in embryonic fibroblasts. *J Biol Chem* 2006;**281**:10715–10726.
27. Ono M, Kubota S, Fujisawa T, Sonoyama W, Kawaki H, Akiyama K *et al*. Promotion of hydroxyapatite-associated, stem cell-based bone regeneration by CCN2. *Cell Transplant* 2008;**17**:231–240.
28. Mestdagh P, Fredlund E, Pattyn F, Rihani A, Van Maerken T, Vermeulen J *et al*. An integrative genomics screen uncovers ncRNA T-UCR functions in neuroblastoma tumours. *Oncogene* 2010;**29**:3583–3592.
29. Betel D, Wilson M, Gabow A, Marks DS, Sander C. The microRNA.org resource: targets and expression. *Nucleic Acids Res* 2008;**36**:D149–D153.
30. Miranda KC, Huynh T, Tay Y, Ang YS, Tam WL, Thomson AM *et al*. A pattern-based method for the identification of MicroRNA binding sites and their corresponding heteroduplexes. *Cell* 2006;**126**:1203–1217.
31. Khwaja A, Rodriguez-Viciana P, Wennström S, Warne PH, Downward J. Matrix adhesion and Ras transformation both activate a phosphoinositide 3-OH kinase and protein kinase B/Akt cellular survival pathway. *EMBO J* 1997;**16**:2783–2793.
32. Lu Q, Rounds S. Focal adhesion kinase and endothelial cell apoptosis. *Microvasc Res* 2012;**83**:56–63.
33. Bellas RE, Harrington EO, Sheahan KL, Newton J, Marcus C, Rounds S. FAK blunts adenosine-homocysteine-induced endothelial cell apoptosis: requirement for PI3-kinase. *Am J Physiol Lung Cell Mol Physiol* 2002;**282**:L1135–L1142.
34. Lim ST, Chen XL, Lim Y, Hanson DA, Vo TT, Howerton K *et al*. Nuclear FAK promotes cell proliferation and survival through FERM-enhanced p53 degradation. *Mol Cell* 2008;**29**:9–22.
35. Ammoun S, Schmid MC, Zhou L, Ristic N, Ercolano E, Hilton DA *et al*. Insulin-like growth factor-binding protein-1 (IGFBP-1) regulates human Schwannoma proliferation, adhesion and survival. *Oncogene* 2011;**31**:1710–1722.
36. Shi-Wen X, Leask A, Abraham D. Regulation and function of connective tissue growth factor/CCN2 in tissue repair, scarring and fibrosis. *Cytokine Growth Factor Rev* 2008;**19**:133–144.
37. Ahmed MS, Gravning J, Martinov VN, von Lueder TG, Edvardsen T, Czibik G *et al*. Mechanisms of novel cardioprotective functions of CCN2/CTGF in myocardial ischemia-reperfusion injury. *Am J Physiol Heart Circ Physiol* 2010;**300**:H1291–H1302.
38. Babic AM, Chen CC, Lau LF. Fisp12/mouse connective tissue growth factor mediates endothelial cell adhesion and migration through integrin alphavbeta3, promotes endothelial cell survival, and induces angiogenesis in vivo. *Mol Cell Biol* 1999;**19**:2958–2966.
39. Chen CC, Lau LF. Functions and mechanisms of action of CCN matricellular proteins. *Int J Biochem Cell Biol.* 2009;**41**:771–783.
40. Guo F, Carter DE, Leask A. Mechanical tension increases CCN2/CTGF expression and proliferation in gingival fibroblasts via a TGFβ-dependent mechanism. *PLoS One* 2011;**6**:e19756.
41. Tan TW, Lai CH, Huang CY, Yang WH, Chen HT, Hsu HC *et al*. CTGF enhances migration and MMP-13 up-regulation via alphavbeta3 integrin, FAK, ERK, and NF-kappaB-dependent pathway in human chondrosarcoma cells. *J Cell Biochem* 2009;**107**:345–356.
42. van Almen GC, Verhesen W, van Leeuwen RE, van de Vrie M, Eurlings C, Schellings MW *et al*. MicroRNA-18 and microRNA-19 regulate CTGF and TSP-1 expression in age-related heart failure. *Aging Cell* 2011;**10**:769–779.
43. Duisters RF, Tijsen AJ, Schroen B, Leenders JJ, Lentink V, van der Made I *et al*. miR-133 and miR-30 regulate connective tissue growth factor: implications for a role of microRNAs in myocardial matrix remodeling. *Circ Res* 2009;**104**:170–178.
44. Knezevic I, Patel A, Sundaresan NR, Gupta MP, Solaro RJ, Nagalingam RS *et al*. A novel cardiomyocyte-enriched microRNA, miR-378, targets insulin-like growth factor 1 receptor: implications in postnatal cardiac remodeling and cell survival. *J Biol Chem* 2012;**287**:12913–12926.